



Removal of Cr(VI) from aqueous solutions by low-temperature biochars from crop residues: role of redox reactions

Qing-Song Liu, Fei Liu, Hong-Han Chen*

School of Water Resources and Environment, China University of Geosciences (Beijing), Beijing 100083, China, Tel. 86-010-82322281; Fax: 86-010-82321081; emails: chenhh@cugb.edu.cn (H.-H. Chen), liukingsong@163.com (Q.-S. Liu), feiliu@cugb.edu.cn (F. Liu)

Received 26 June 2016; Accepted 19 November 2016

ABSTRACT

Biochars were prepared from a series of crop residues at 250°C and tested for their Cr(VI) removal performance. At low pHs, Cr(VI) was reduced to Cr(III) and adsorbed favorably through complexation. The maximum adsorption capacities of total Cr were in a range of 41.2–133.7 mg/g at pH 2.5. Total Cr adsorption was correlated with the reducing capacities of biochars. Studies on pH, temperature and ionic strength effects proved the dependency of total Cr adsorption on Cr(VI) reduction. Cr(VI) reduction occurred on biochar surface after binding through electrostatic force. By comparison, direct Cr(III) adsorption from solution was through electrostatic force and surface complexation, which was inferior and susceptible to proton competition. Based on Fourier transform infrared spectroscopy and X-ray photoelectron spectroscopy analysis, alcohols and phenolic groups were oxidized to carboxyl and carbonyl groups in redox reactions. As a result, the role of redox reactions was explained as follows: (1) the functional groups are more accessible for Cr(III) converted on biochar surface and (2) the newly created functional groups readily participate in Cr(III) complexation.

Keywords: Adsorption; Reduction; Chromium; Inner-sphere complexation; Mechanisms

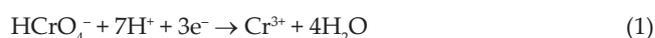
1. Introduction

Biochar is a carbon-rich material produced from the pyrolysis of biomass. With abundant surface functional groups and inorganic components [1], it is capable of effectively alleviating a variety of contaminants from water. Hence, biochar can serve as an effective and low-cost adsorbent for wastewater treatment. The removal of various heavy metals by biochars such as Pb(II), Ni(II), Cu(II) and Cr(VI) has proved to be favorable [2–6].

Various biomass sources have been applied to prepare biochars such as wood [7], municipal waste [8], animal manure [9] and crop residues [10]. A large number of crop residues are annually generated in China, most of which are not well utilized. In fact, crop residues comprise an abundant, economical and stable supply for biochar production. Several crop residues have been tested to prepare biochars

aimed at heavy metal removal, such as corn straw [3], wheat straw [11], peanut husk [12] and sesame straw [13].

Chromium is used in industries such as electroplating, dyes and pigments, tanning, and wood preserving [14]. In natural environment, chromium exists in two stable oxidation state: Cr(VI) and Cr(III). The former is of particular concern due to its greater toxicity and mobility. Cr(VI) is commonly removed by precipitation after its reduction to Cr(III). Recently, several studies dealing with the removal of Cr(VI) with biochars have been reported [6,15–17]. It is established that the adsorption of Cr(VI) onto biochars, as well as other biomaterials, involves its reduction to Cr(III) and the subsequent binding of Cr(III). The reduction of Cr(VI) could be expressed as Eq. (1):



In most cases, the resultant Cr(III) is favorably adsorbed after Cr(VI) reduction. However, the correlation between

* Corresponding author.

Cr(VI) reduction and total Cr adsorption has not been well understood. Chen et al. [15] observed that Cr(VI) adsorption onto biochar is quite inferior without its reduction to Cr(III). Dupont et al. [18] pointed out that Cr(VI) adsorption requires its reduction to Cr(III). Two reasons might be responsible for the favorable adsorption of converted Cr(III): (1) since Cr(VI) reduction is a surface reaction, the converted Cr(III) reaches functional groups readily and forms complexes with them and (2) the functional groups would be changed in redox reactions, which has implications on Cr(III) binding. Here, a specific study is needed to test these assumptions.

In this study, five types of biochars were prepared from crop residues at low temperature (250°C). The abundance of feedstock and the low pyrolysis temperature reduce the cost of biochar production. Their adsorption characteristics toward Cr(VI) have been studied. The role played by redox reactions was specially examined. A deep understanding of the role played by redox reactions helps us to improve the efficiency of Cr(VI) removal using biochars.

2. Materials and methods

2.1. Materials and chemicals

Crop residues including corncob, maize straw, wheat straw, cotton stalk and peanut hull were all collected from Wuqiao County, Hebei Province, China. Analytical grade $K_2Cr_2O_7$ was purchased from Sinopharm Chemical Reagent Co., Ltd., Shanghai, China. All other chemicals were of analytical grade. Distilled water was used in this study.

2.2. Preparation of biochars

Crop residues were firstly washed repeatedly, dried at 80°C, ground with a high-speed grinder and sieved to 180–850 μm particle size. Then, 10.0 g material was put into a 50-mL ceramic crucible covered with a lid and heated in a muffle furnace under oxygen-limited condition (SGM. M6, Xigema, Luoyang, China) at 250°C for 2 h (heating rate 4°C/min). Afterward, the resulting biochars were cooled to room temperature in the furnace and stored in airtight containers. Based on the feedstock, the obtained biochars were denoted as CCB (corncob), MSB (maize straw), WSB (wheat straw), CSB (cotton stalk) and PHB (peanut hull). The biochar yield (%) was the mass percent of biochar to its raw material on dry basis.

2.3. Characterization methods

Ash content was measured by heating biochar samples at 750°C for 6 h. Surface area was obtained by the Brunauer–Emmett–Teller (BET) method conducted with a Micromeritics ASAP 2020 (Micromeritics, Norcross, GA, USA). Cation exchange capacity (CEC) was measured based on a modified NH_4 -acetate compulsory displacement method [19]. Point of zero charge (pH_{PZC}) was determined by a mass titration method proposed by Noh and Schwarz [20]. The analysis of acidic surface functional groups (SFGs) was based on a modified Boehm titration method [21].

The Fourier transform infrared spectroscopy (FTIR) analysis was conducted with a Nicolet Nexus 670 (Thermo Nicolet,

Madison, WI, USA). Biochar was mixed with KBr powder and pressed into pellets. The spectra were recorded from 4,000 to 400 cm^{-1} ; scans were taken at a resolution of 2 cm^{-1} .

The X-ray photoelectron spectroscopy (XPS) analysis was conducted using a PHI5700 ESCA system (Physical Electronics, Chanhassen, MN, USA) equipped with an Al $K\alpha$ X-ray source (1,486.6 eV). Pass energy was set as 178.95 and 22.35 eV for survey and high-resolution spectra, respectively. The spectra were calibrated by taking the graphitic peak as 284.6 eV. Atomic ratios were calculated from survey spectra by correcting the peak areas based on sensitivity factors. The high-resolution spectra were analyzed using the XPSPEAK software, based on the Gaussian:Lorentzian (80%:20%) function after baseline subtraction with Shirley method.

2.4. Adsorption procedure

The adsorption of Cr(VI) from aqueous solutions onto biochars was conducted by batch mode in stoppered flasks. In equilibrium studies, 0.100 g biochar was mixed with 100 mL solution and shaken in a rotary shaking incubator (HZS-280, Peiying, Taicang, China) at 25°C and 150 rpm. Based on preliminary tests, the contact time was set as 21 d to ensure equilibrium. The initial concentration range of Cr(VI) was 10–100 mg/L, obtained by the dilution of 1,000 mg/L stock solution. The equilibrium pH was regulated via the addition of HNO_3 (1 mol/L for pH 1.6 and 2.5 and 0.001 mol/L for pH 5.5), whose amount was predetermined. After contact, the supernatant was filtrated with 0.45 μm membrane filters, followed by the analysis of Cr(VI) and total Cr. Control experiments without biochar addition were conducted and detected no measurable change in Cr(VI) concentration. All the experiments were performed in duplicate. The uptake of total Cr at equilibrium, q_e (mg/g), was calculated by the following equation:

$$q_e = V(C_0 - C_e)/m \quad (2)$$

where C_0 is the initial concentration of Cr (mg/L); C_e is the equilibrium concentration of total Cr (mg/L); V is the volume of solution (L); and m is the weight of biochar (g).

In kinetic studies, 0.200 g biochar was mixed with 200 mL solution. The initial concentration was set as 100 mg/L. Solution pH was set as 2.5. Samples were taken at desired time intervals and filtered immediately. The uptake of total Cr at time t , q_t (mg/g), was calculated by the following equation:

$$q_t = V(C_0 - C_t)/m \quad (3)$$

where C_t is the concentration of total Cr at time t (mg/L).

The release of cations in Cr(VI) adsorption was analyzed. The initial concentration was 100 mg/L, and solution pH was set as 2.5. At equilibrium, the supernatant was filtrated with 0.45 μm membrane filters, followed by the analysis of various cations (inductively coupled plasma with atomic emission spectroscopy, NexION 300X, PerkinElmer, Waltham, MA, USA). Blank experiments were conducted followed a similar procedure at the absence of Cr(VI). The difference between the presence and absence of Cr(VI) was taken as the net release amount. For comparison, the release of cations in Cr(III) adsorption was also analyzed, which followed a

similar procedure as Cr(VI) adsorption except that solution pH was set as 4.2.

The analysis of Cr species was through colorimetric method using a spectrophotometer (UV-1200, Mapada, Shanghai, China). Cr(VI) reacts with 1,5-diphenylcarbazide in acidic solution to form a pink complex, which was analyzed colorimetrically at 540 nm. Total Cr was measured similarly after Cr(III) was converted to Cr(VI) through KMnO_4 oxidation under acidic condition. Cr(III) was the difference between total Cr and Cr(VI).

2.5. Data analysis

Adsorption isotherms were fitted to the Langmuir and Freundlich models. The Langmuir model can be written as:

$$q_e = q_m K_L C_e / (1 + K_L C_e) \quad (4)$$

where q_m is the maximal adsorption capacity (mg/g), and K_L is a constant related to the free energy of the adsorption (L/mg).

The Freundlich model can be written as:

$$q_e = K_F C_e^{1/n} \quad (5)$$

where K_F and $1/n$ (unit-less) are constants related to the adsorption capacity and intensity, respectively.

Adsorption kinetics were fitted to the pseudo-first-order, pseudo-second-order and intraparticle diffusion models. The pseudo-first-order model can be expressed as:

$$\ln(q_e - q_t) = \ln q_e - k_1 t \quad (6)$$

where k_1 is the first-order rate constant.

The pseudo-second-order model can be expressed as:

$$\frac{t}{q_t} = \frac{1}{k_2 q_e^2} + \frac{t}{q_e} \quad (7)$$

where k_2 is the second-order rate constant.

The intraparticle diffusion model can be expressed as:

$$q_t = k_{id} t^{1/2} + C \quad (8)$$

where k_{id} is the intraparticle diffusion constant, and C is a parameter related to the boundary layer effect.

3. Results and discussion

3.1. Biochar properties

Some properties of various biochars are summarized in Table 1. The yields of biochars were in a range of 41.6%–47.4%. The ash contents were in a range of 4.75%–13.12%. The surface areas of all biochars were quite low (<3 m²/g). The pH_{PZC} values varied in a wide range from 4.30 to 7.25. The total bases were in a narrow range of 1.02–1.27 meq/g. Substantial amounts of acidic SFGs were present in biochars, with sums of 3.15–6.28 meq/g. Notable variations were observed in SFGs with different acidic strengths among various biochars. It should be mentioned that the results represented the potential amounts of SFGs, since all acidic sites were protonated in the pretreatment. The CEC values differed substantially in a range of 32.2–127.0 cmol/kg.

3.2. Effects of pH

The adsorption isotherms of total Cr on biochars at various pHs are illustrated in Fig. 1. Obviously, the affinities of biochars toward total Cr, including Cr(VI) and Cr(III), depended strongly on pH and biochar type. Total Cr adsorption at pH 5.5 was rather inferior, with maximum experimental uptakes below 20 mg/g. The adsorption was remarkably improved at pH 2.5, with experimental uptakes in the range of 37.2–83.9 mg/g. As pH decreased to 1.6, the uptakes were decreased moderately in low concentration range, but reached to similar or enhanced levels in high concentration range. At low pHs, the adsorption capacities of biochars followed the order of WSB > CSB ≈ PHB > MSB > CCB.

The Langmuir and Freundlich models were applied to fit the experimental data, and the fitting parameters are listed in Table 2. The Langmuir model was generally more suitable, with correlation coefficients (R^2) above 0.94. The maximum adsorption capacities (q_m) obtained at pH 2.5, in the range of 41.2–133.7 mg/g, followed the same order as experimental data. The q_m values were compared with those of other biochars [6,15–17], as well as lignocellulosic materials [22]. Consequently, the low-cost biochars used in this study showed higher or comparable adsorption capacities than most biochars and lignocellulosic materials.

To ascertain the chemical state of bounded Cr, XPS high-resolution spectra of Cr 2p orbitals from Cr(VI)-laden biochars were obtained, as shown in Fig. 2. Two strong bands appeared at binding energies of 574.0–578.0 and 586–588.0 eV, corresponding to Cr 2p_{3/2} and Cr 2p_{1/2} orbitals, respectively. The Cr 2p_{3/2} peak was analyzed by assuming that the binding energies center at 577.3 and 579.5 eV for Cr(III) and Cr(VI),

Table 1
Properties of various biochars

Biochars	Yields (%)	Ash (%)	S_{BET} (m ² /g)	pH_{PZC}	Total bases (meq/g)	Acidic SFGs (meq/g)				CEC (cmol/kg)
						Carboxylic	Lactonic	Phenolic	Total	
CCB	46.3	5.56	1.15	4.30	1.10	1.69	0.81	1.02	3.52	67.2
MSB	44.6	7.91	1.21	7.25	1.19	1.14	1.36	0.72	3.22	87.5
WSB	44.0	13.12	2.17	4.50	1.27	1.54	3.56	1.18	6.28	127.2
CSB	41.6	4.75	0.12	5.30	1.19	1.54	0.96	1.28	3.78	105.7
PHB	47.4	8.92	1.28	6.15	1.02	0.79	1.06	1.30	3.15	32.2

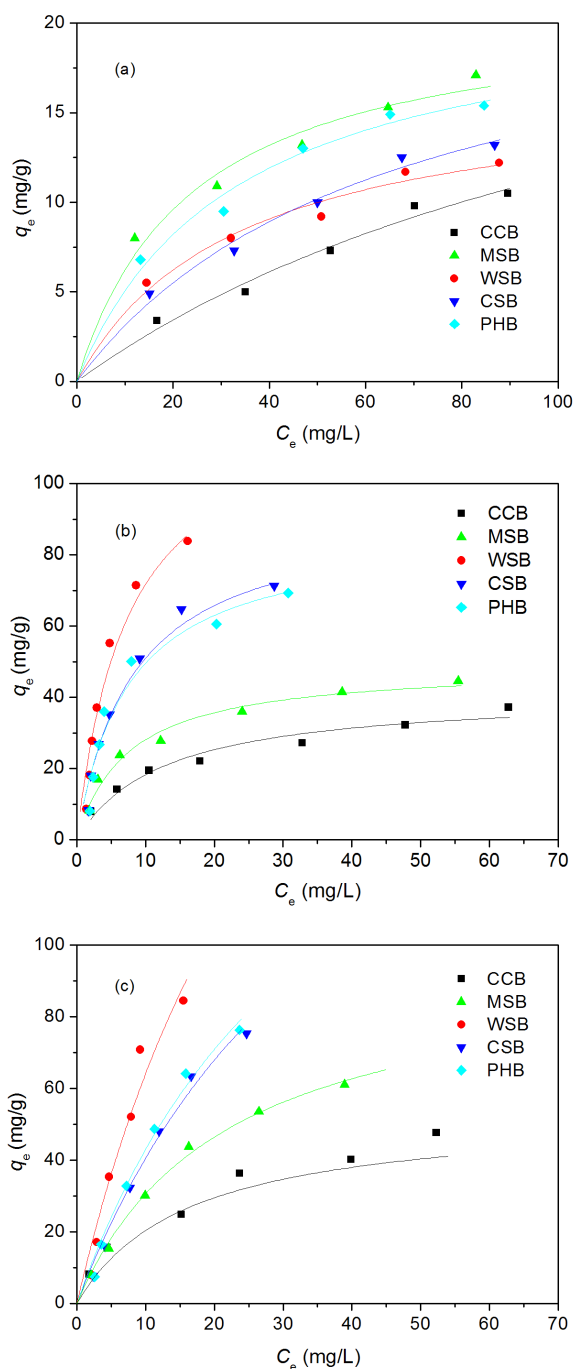


Fig. 1. Adsorption isotherms of total Cr onto biochars at 25°C: (a) pH 5.5; (b) pH 2.5 and (c) pH 1.6.

respectively [23]. Their relative compositions are given in Fig. 2. At pH 5.5, Cr(III) was the main component of bounded Cr (>58.2%), while Cr(VI) also made a considerable contribution. At pH 2.5, Cr(III) was the predominant species of bounded Cr, with ratios in the range of 85.8%–96.4%.

The aqueous concentrations of Cr species at various pHs are presented in Fig. 3. Due to its intense removal through surface complexation and/or precipitation, aqueous Cr(III) was not detected at pH 5.5. Aqueous Cr(III) was detected at

Table 2
Isotherm fitting parameters with the Langmuir and Freundlich models

Biochars	pH	Langmuir			Freundlich		
		q_m (mg/g)	K_L (L/mg)	R^2	K_F (mg/g) (L/mg) ^{1/n}	n	R^2
CCB	5.5	27.69	0.0071	0.974	0.409	1.370	0.976
	2.5	41.23	0.0793	0.958	6.872	2.475	0.991
	1.6	53.37	0.0615	0.967	7.302	2.110	0.981
MSB	5.5	21.02	0.0420	0.952	2.836	2.473	0.997
	2.5	48.98	0.134	0.979	10.01	2.591	0.955
	1.6	209.4	0.0240	0.988	6.267	1.260	0.975
WSB	5.5	16.71	0.0297	0.959	1.642	2.211	0.977
	2.5	133.7	0.118	0.951	17.67	1.697	0.898
	1.6	180.5	0.0493	0.943	10.67	1.377	0.909
CSB	5.5	23.48	0.0153	0.981	0.983	1.695	0.982
	2.5	92.43	0.123	0.969	15.59	2.144	0.891
	1.6	96.40	0.0465	0.994	7.524	1.704	0.970
PHB	5.5	21.70	0.0304	0.971	2.128	2.195	0.968
	2.5	86.32	0.135	0.945	15.34	2.196	0.883
	1.6	202.8	0.0269	0.984	6.763	1.275	0.970

low pHs, while Cr(VI) made up an ever-larger fraction with the increase of initial concentration. Aqueous Cr(III) was kept at low levels at pH 2.5, indicating its favorable adsorption on biochars. As pH decreased to 1.6, aqueous Cr(VI) decreased remarkably, coupled with an increase in aqueous Cr(III).

At pH 5.5, Cr(VI) reduction was attenuated heavily due to the limitation of protons. However, as suggested by XPS spectra, the occurrence of Cr(III) was crucial for the overall adsorption. At low pHs, inner-sphere complexation between converted Cr(III) and functional groups on biochars was considered to be dominant [6,16]. Meanwhile, the unreduced Cr(VI), in the form of HCrO_4^- , was bounded on the positively charged biochar through electrostatic attraction. Under strongly acidic conditions, Cr(VI) reduction was dominated by the abundance of electron donors. To evaluate the reducing capacities of biochars, the conversion rates of Cr(VI) were calculated at pH 2.5 and $C_0 = 100$ mg/L. The results were 46.8%, 50.2%, 85.3%, 74.1% and 73.9% for CCB, MSB, WSB, CSB and PHB, respectively. Consequently, the adsorption capacities of biochars were well correlated with their reducing capacities, i.e., the stronger in reducing capacities, the higher in adsorption capacities.

3.3. Effects of temperature and ionic strength

The adsorption isotherms of total Cr at different temperatures are presented in Fig. 4. Compared with 25°C, total Cr adsorption at 15°C was remarkably inferior over the whole concentration range. At 35°C, total Cr adsorption decreased slightly in low concentration range, but reached to similar or higher levels in high concentration range. Enhancement of Cr adsorption with temperature was observed in previous studies, which was attributed to the endothermic nature of the adsorption [24,25]. An increase in temperature promotes

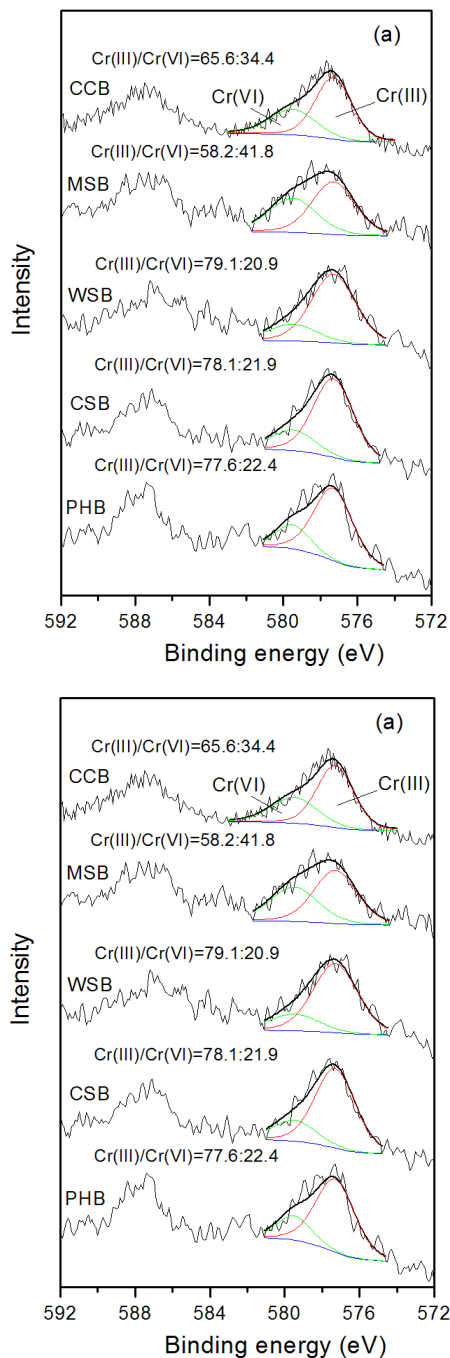


Fig. 2. High-resolution Cr 2p spectra of Cr(VI)-laden biochars prepared at 25°C, $C_0 = 100$ mg/L: (a) pH 5.5 and (b) pH 2.5.

diffusion, which benefits Cr adsorption. In addition, the role played by redox reactions should be given attention. The aqueous concentrations of Cr species at different temperatures are recorded in Fig. 5. Compared with 25°C, aqueous Cr(VI) was significantly higher at 15°C. Thus, Cr(VI) adsorption in its anionic form was not so favorable. The disparity in Cr adsorption between the two temperatures was derived mainly from the dependency of redox reactions on temperature. As temperature increased to 35°C, aqueous Cr(VI) was

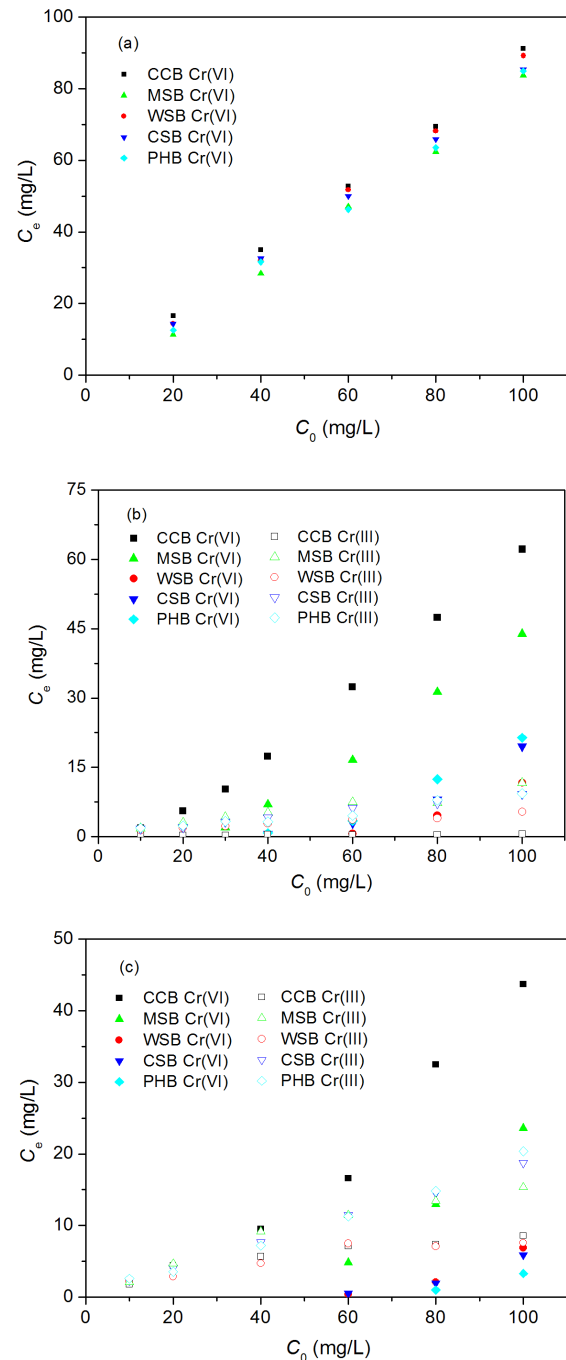


Fig. 3. Equilibrium concentrations of Cr species in solution at 25°C: (a) pH 5.5; (b) pH 2.5; and (c) pH 1.6.

further decreased, meanwhile aqueous Cr(III) showed an increase. The enhancement in Cr(VI) reduction favors the overall adsorption, especially in high concentration range.

Ionic strength is another important factor in the adsorption of heavy metals from solutions. Its influences on Cr adsorption are demonstrated in Fig. 6. For each biochar, Cr adsorption was slightly affected at ionic strength 0.1 M, but a notable decrease was observed at 1 M. An increase in ionic strength influenced Cr adsorption in two respects:

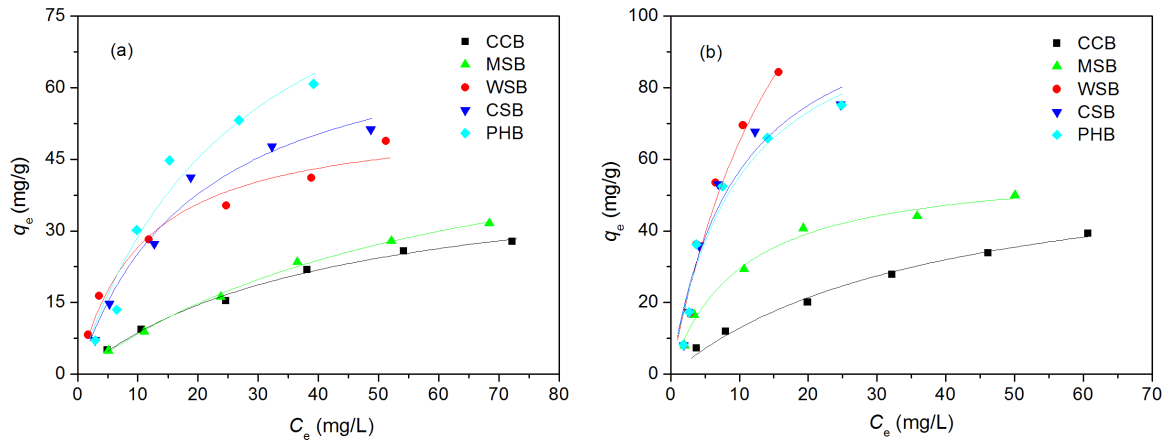


Fig. 4. Adsorption isotherms of total Cr onto biochars at pH 2.5: (a) 15°C and (b) 35°C.

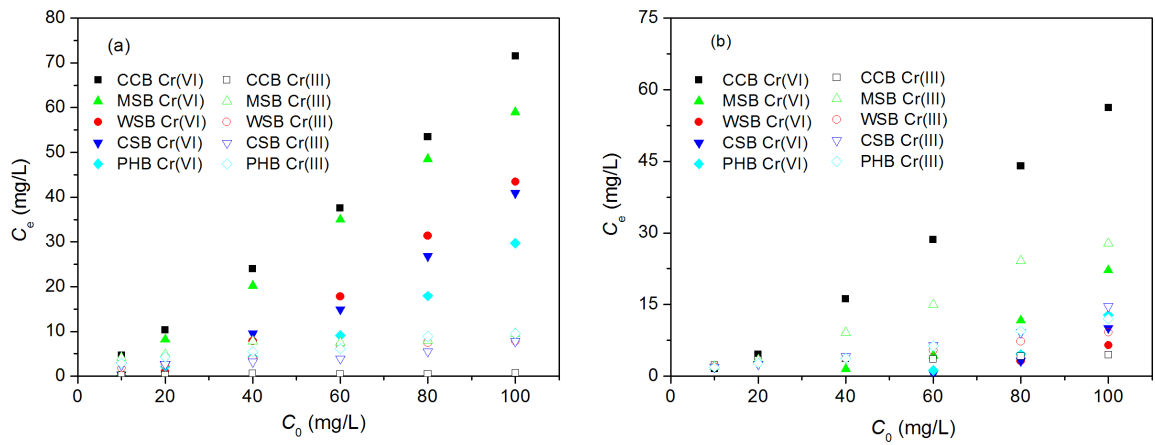


Fig. 5. Equilibrium concentrations of Cr species in solution at pH 2.5: (a) 15°C and (b) 35°C.

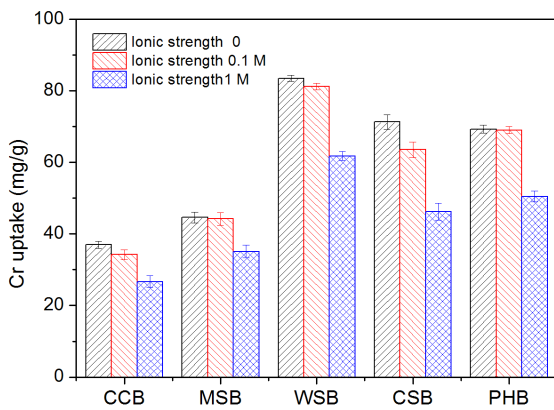


Fig. 6. Effects of ionic strength on the adsorption of total Cr onto biochars, conditions: 25°C, pH 2.5, and $C_0 = 100$ mg/L.

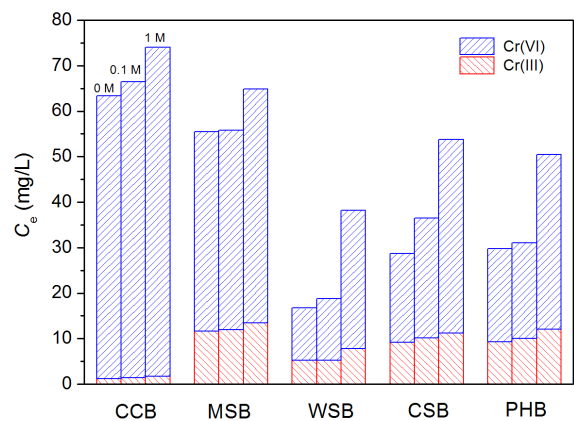


Fig. 7. Equilibrium concentrations of Cr species in solution at various ionic strengths, conditions: 25°C, pH 2.5, and $C_0 = 100$ mg/L.

(1) the electrostatic attraction between Cr(VI) and biochars was attenuated due to the screening effects of added salt and (2) the cations competed with Cr(III) for the active sites. The effects of ionic strength on aqueous Cr species are shown in Fig. 7. The increase in aqueous Cr(III) was minor when ionic

strength was increased to 1 M. Meanwhile, the increase in aqueous Cr(VI) was more significant. Hence, the effects of ionic strength were ascribed mainly to the attenuation in Cr(VI) reduction. The interactions between Cr(III) and biochars were strong and resistant to the competition from other

cations. Accordingly, specific interactions rather than electrostatic interactions dominated Cr(III) binding.

3.4. Adsorption kinetic studies

The adsorption kinetic curves of total Cr are given in Fig. 8. The adsorption was slow, but the uptake increased steadily over a long time. It took at least 360 h to reach equilibrium. The adsorption process was proposed as: (1) mass transfer of Cr(VI) to biochar surface; (2) contact with electron donors and conversion to Cr(III) and (3) binding of Cr(III). There existed electrostatic attraction between Cr(VI) and biochar, which favored the first stage. The second stage was the rate-limiting step. The continuous consumption of electron donors and Cr(VI) anions diminished their contact chances and the reaction rate. The last stage was a rapid process.

The adsorption kinetics are fitted to various models, and the parameters are listed in Table 3. The pseudo-first-order model was inapplicable for most cases. The pseudo-second-order model showed an acceptable fit for each case, with calculated q_e values close to the experimental results. The applicability of this model is an indication of chemisorption in nature [26], which is consistent with the reduction and complexation of Cr(VI). The intraparticle diffusion model gave satisfactory fit for all cases. A good linearity of the fitting line was observed for each case over the entire time range, indicating the dominance of intraparticle diffusion (fitting lines are plotted in Fig. S1, see supporting materials).

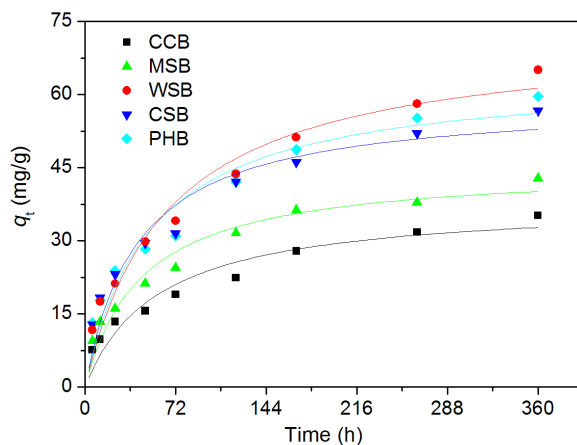


Fig. 8. Adsorption kinetics of total Cr onto biochars at 25°C, pH 2.5, and $C_0 = 100$ mg/L.

Table 3
Kinetic fitting parameters with various models

Biochars	Pseudo-first-order			Pseudo-second-order			Intraparticle diffusion		
	k_1 (h^{-1})	q_e (mg/g)	R^2	$k_2 \times 10^4$ ($\text{g} \cdot \text{mg}^{-1} \cdot \text{h}^{-1}$)	q_e (mg/g)	R^2	k_{id} ($\text{mg} \cdot \text{g}^{-1} \cdot \text{h}^{-0.5}$)	C (mg/g)	R^2
CCB	0.0137	32.4	0.868	4.54	38.0	0.936	1.684	4.249	0.991
MSB	0.0175	39.0	0.901	4.87	45.2	0.948	2.024	6.724	0.971
WSB	0.0133	60.5	0.925	2.11	72.5	0.959	3.245	6.157	0.990
CSB	0.0184	51.3	0.875	4.08	58.9	0.938	2.644	9.619	0.978
PHB	0.0152	55.3	0.877	3.00	64.2	0.929	2.864	8.369	0.984

The evolution of aqueous Cr(III) with time is demonstrated in Fig. 9. Cr(III) was detected in solution at the start, which increased during a short period and almost stabilized afterward, although the adsorption and reduction of Cr(VI) continued for a long time. Direct and indirect mechanisms have been proposed to explain the removal of Cr(VI) by biomaterials [27]. According to the direct mechanism, Cr(VI) reduction occurs in solution, then the converted Cr(III) forms complexes with biomaterials or remains in solution. If this was true in this study, the migration of Cr(III) from solution onto biochar surface would be difficult, considering the strong electrostatic repulsion between them. As a result, the indirect mechanism should be dominant in this study, i.e., Cr(VI) reduction and adsorption occur mainly on biochar surface.

3.5. Comparison with Cr(III) adsorption

Based on previous results, total Cr adsorption tended to be favored when the redox reactions were enhanced. To explore the role of redox reactions, the adsorption behaviors of Cr(VI) and Cr(III) were compared, as shown in Fig. 10. At pH 3.2, Cr(III) uptakes were below 10 mg/g for all biochars. At pH 4.2, the uptakes were increased but still not comparable with Cr(VI) adsorption (as a starting species). Obviously, Cr(III) adsorption from solution onto biochars was inferior and susceptible to proton competition. In contrast, proton competition was not prominent in

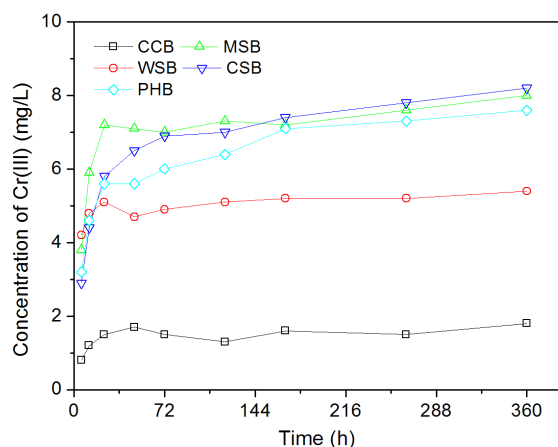


Fig. 9. Evolution of aqueous Cr(III) as a function of time at 25°C and pH 2.5.

Cr(VI) adsorption even at pH 1.6, although the bounded Cr species was primarily Cr(III). An important reason for their different performance lay in the accessibilities to functional groups. As Cr(VI) reduction proceeded on biochar surface, the functional groups were adjacent to the converted Cr(III). On the other hand, Cr(III) ion in solution must overcome repulsive force before reaching the functional groups.

The net release of various cations in Cr(III) and Cr(VI) adsorptions was analyzed, as summarized in Table 4. For Cr(III) adsorption, the net release of various cations were positive. Accordingly, ion exchange was involved in Cr(III) adsorption, especially for biochars with high CECs, i.e., WSB and CSB. It was calculated that ion exchange accounted for 10.3%, 9.3%, 48.5%, 64.9% and 15.0% of Cr(III) uptakes on CCB, MSB, WSB, CSB and PHB, respectively. For Cr(VI) adsorption, the net release of Ca and Mg were negative, suggesting that their release was attenuated at the presence of Cr(VI). This unexpected phenomenon was attributed to the increase in active sites. The results proved the minimal role of ion exchange in Cr(VI) adsorption. In fact, the disparity between Cr adsorption capacities and CECs of biochars also supported this point.

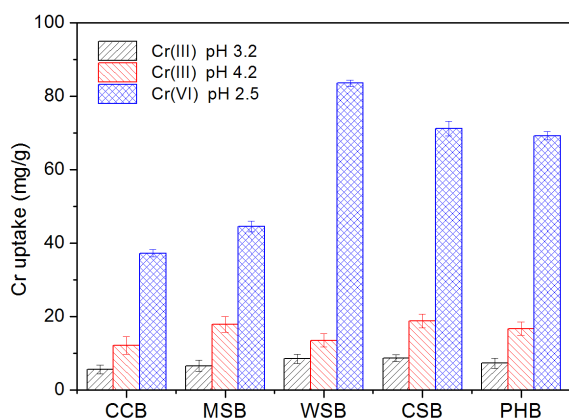


Fig. 10. Comparisons between Cr(VI) and Cr(III) adsorption: conditions: 25°C and $C_0 = 100$ mg/L.

Table 4

Net release of cations in Cr(III) and Cr(VI) adsorptions (meq/g)

Biochars	Adsorbates	Ca	Mg	2K	2Na
CCB	Cr(III)	0.007 ± 0.001	0.012 ± 0.002	0.010 ± 0.002	0.006 ± 0.001
	Cr(VI)	-0.024 ± 0.011	-0.034 ± 0.007	— ^a	0.004 ± 0.001
MSB	Cr(III)	0.008 ± 0.002	0.022 ± 0.004	0.014 ± 0.002	0.005 ± 0.001
	Cr(VI)	-0.048 ± 0.016	-0.148 ± 0.010	—	0.003 ± 0.001
WSB	Cr(III)	0.028 ± 0.009	0.103 ± 0.009	0.047 ± 0.009	0.010 ± 0.002
	Cr(VI)	-0.029 ± 0.009	-0.081 ± 0.010	—	0.003 ± 0.001
CSB	Cr(III)	0.071 ± 0.014	0.201 ± 0.014	0.012 ± 0.003	0.068 ± 0.007
	Cr(VI)	-0.013 ± 0.014	-0.041 ± 0.010	—	0.003 ± 0.001
PHB	Cr(III)	0.009 ± 0.002	0.021 ± 0.003	0.014 ± 0.003	0.027 ± 0.005
	Cr(VI)	-0.056 ± 0.020	-0.118 ± 0.009	—	0.005 ± 0.001

^aThe release of K in Cr(VI) adsorption was not analyzed due to the use of $K_2Cr_2O_7$. The added K was equivalent to 1.923 meq/g.

However, electrostatic repulsion alone could not be explained for the inferior adsorption of Cr(III) compared with Cr(VI). Cr(III) adsorption was tested at pH 4.2, which was close to the pH_{PZC} of CCB and WSB. In these cases, the repulsive force was not so strong to notably reduce Cr(III) adsorption. It was reasonable to presume that additional active sites were created in Cr(VI) reduction. The decreased release of divalent metals in Cr(VI) adsorption provided evidence for this presumption. The change of functional groups in redox reactions will be analyzed in the following section.

3.6. Involvement of functional groups

FTIR and XPS analysis were employed to study the functional groups. Cr(VI)- and Cr(III)-laden biochars were prepared at pH 2.5 and 4.2, respectively. Pristine biochars were prepared for comparison, which underwent a similar procedure at pH 2.5 at the absence of Cr.

The FTIR spectra of various samples are illustrated in Fig. 11. For WSB, the broad band at 3413 cm^{-1} was assigned to the $-OH$ stretching vibration. The prominent band at 2925 cm^{-1} was attributed to aliphatic $-CH_2$ stretching vibration. The notable band at 1705 cm^{-1} was derived from the

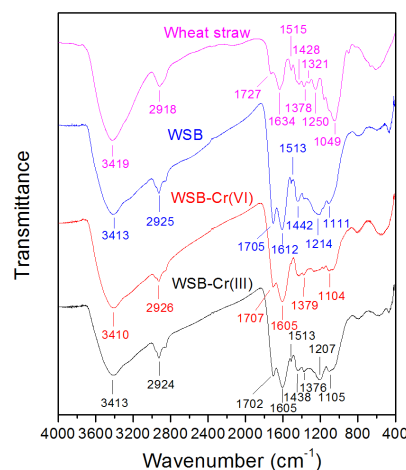


Fig. 11. FTIR spectra of pristine and Cr-laden WSBs.

–COOH stretching vibration [28,29]. The strong band at 1,612 cm^{-1} , the weak band at 1,513 cm^{-1} and the medium band at 1,442 cm^{-1} were related to the aromatic ring [30,31]. The bands at 1,214 and 1,111 cm^{-1} corresponded to the C–O stretching vibration [32,33]. WSB retained some characteristics of its feedstock (wheat straw), but some differences were obvious between them. The –COOH related band was more intense for WSB, suggesting its formation during pyrolysis. The positions of aromatic ring related bands in WSB shifted from those of wheat straw. The intensities and positions of two bands at 1,250 and 1,049 cm^{-1} in wheat straw, associated with C–O–C in ether and –CH₂OH in alcohols, changed significantly after pyrolysis.

For Cr(VI)-laden WSB, the intensity of –OH band (3,410 cm^{-1}) did not change notably, but its position shifted slightly. The aliphatic –CH₂ related band (2,926 cm^{-1}) was moderately attenuated. The –COOH related band (1,707 cm^{-1}) was notably diminished. The bands at 1,513 and 1,442 cm^{-1} in WSB, corresponding to aromatic ring, were hardly discernible. The C–O related band (1,214 cm^{-1}) disappeared. For Cr(III)-laden WSB, the –OH and aliphatic –CH₂ related bands did not change from those of WSB. The –COOH related band was also diminished, but not so strong as Cr(VI)-laden WSB. The aromatic ring related bands were similar to those of WSB. The C–O related band (1,207 cm^{-1}) was basically retained.

The surface elemental compositions of various samples based on XPS have been given in Table 5. Compared with the pristine biochars, the oxygen contents of the Cr(VI)-laden biochars showed remarkable increases, indicating that the surface functional groups underwent notable changes during Cr(VI) reduction. To get further insight into the variation of functional groups, the high-resolution spectra of C1s are given in the analysis. Three components are considered with chemical shifts as follows [34]: graphite (284.6 eV), C–OH (286.1 \pm 0.1 eV) and C=O (288.2 \pm 0.1 eV). The results are also given in Table 5 (the fitting lines are shown in Fig. S2).

Based on the results, the C–OH related groups were remarkably decreased for all Cr(VI)-laden biochars, indicating their involvement in Cr(VI) reduction. Meanwhile, the C=O related groups showed an increase except for Cr(VI)-laden MSB, suggesting that C–O bond was oxidized to C=O bond in redox reactions. In contrast, the oxygen contents and C1s components of Cr(III)-laden biochars were similar to those of pristine biochars.

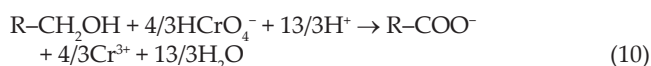
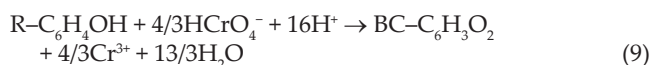
Cellulose, hemicellulose and lignin are the main moieties of lignocellulosic materials [35]. According to the FTIR analysis, the C–O related groups in cellulose and hemicellulose were remarkably altered after pyrolysis, while the aromatic structure in lignin was affected to some extent. The aromatic structure was altered in Cr(VI)-laden biochar, suggesting their involvement in Cr(VI) reduction. The disappearance of C–O related groups indicated their role as electron donors in Cr(VI) donors. They were probably phenolic hydroxyl groups in lignin and alcohols in cellulose and hemicellulose. The consumption of alcohols was supported by the attenuation of aliphatic –CH₂ in Cr(VI)-laden biochar. The participation of C–O related groups in Cr(VI) reduction was verified by the XPS analysis, which further illustrated the formation of C=O related groups. The newly formed groups were probably carboxyl and carbonyl groups, which supplied more active sites for Cr(III) complexation. In contrast, the consumption of aromatic structure and C–O related groups, as well as the formation of C=O related groups, were not observed for Cr(III)-laden biochar.

The intensity of carboxylic group related band in FTIR spectra was indeed diminished in Cr(VI)-laden biochar, but the same phenomenon, to a lesser extent, was observed in Cr(III)-laden biochar. Moreover, the reducing capacities of biochars were not consistent with their surface density of carboxylic groups. Hence, carboxylic groups acted as ligands in Cr(III) complexation rather than electron donors in Cr(VI) reduction. Additionally, –OH in phenolic groups were possibly involved in Cr(III) complexation.

Table 5
Surface elemental composition and C1s analysis based on XPS

Samples	Surface elemental compositions (%)					Curve fitting of C1s (%)		
	C	O	N	Si	Cr	C–C	C–OH	C=O
CCB	75.88	21.77	0.80	1.55	–	72.4	20.3	7.2
CCB–Cr(VI)	67.32	28.45	0.74	–	3.49	87.4	3.4	9.2
CCB–Cr(III)	74.60	22.70	1.29	–	1.40	70.2	22.0	7.7
MSB	78.76	18.76	1.85	0.63	–	66.4	22.9	10.7
MSB–Cr(VI)	70.13	25.63	1.15	–	3.08	77.2	12.9	9.9
MSB–Cr(III)	77.55	19.17	1.62	–	1.65	67.9	22.5	9.6
WSB	77.48	20.31	1.80	0.41	–	75.6	19.9	4.5
WSB–Cr(VI)	75.45	22.30	1.82	–	1.43	79.7	13.4	6.9
WSB–Cr(III)	76.12	20.69	1.93	–	0.97	78.1	13.6	8.4
CSB	78.76	19.39	1.54	0.30	–	70.5	19.8	9.7
CSB–Cr(VI)	65.11	28.63	0.98	–	4.44	77.5	10.9	11.6
CSB–Cr(III)	77.01	19.50	1.68	–	1.81	69.7	21.3	9.0
PHB	78.03	19.46	2.26	0.25	–	70.6	22.6	6.8
PHB–Cr(VI)	76.67	20.55	1.49	–	1.29	79.7	12.3	8.0
PHB–Cr(III)	77.20	19.50	2.50	–	0.80	68.6	23.0	8.4

The possible reactions in Cr(VI) reduction were recommended in Eqs. (9) and (10):



4. Conclusions

This study demonstrated the applicability of low-cost biochars for Cr(VI) removal, and the importance of redox reactions in the adsorption of total Cr. The removal of Cr(VI) was related to biochar type, pH, temperature, ionic strength and Cr(VI) initial concentration. An interrelation was found between Cr(VI) reduction and total Cr adsorption. The adsorption isotherms followed Langmuir model, while adsorption kinetics could be fitted by the pseudo-second-order and intraparticle diffusion models. A comparison with Cr(III) adsorption proved the superiority of reduction-coupled adsorption of Cr(VI). Spectra analysis illustrated the involvement and alteration of some groups in Cr(VI) reduction and Cr(III) complexation. Redox reactions not only reduces the toxicity of Cr(VI) but also facilitate the complexation of Cr(III). In practical application, attention should be given to create favorable conditions for Cr(VI) reduction.

Acknowledgments

The authors appreciate the financial support by the Natural Science Foundation of China (No. 21407130), the Fundamental Research Funds for the Central Universities (No. 2652015129) and the China Scholarship Council.

References

- [1] Z.Y. Wang, G.C. Liu, H. Zheng, F.M. Li, H.H. Ngo, W.S. Guo, C. Liu, L. Chen, B.S. Xing, Investigating the mechanisms of biochar's removal of lead from solution, *Bioresour. Technol.*, 177 (2015) 308–317.
- [2] Y.P. Qiu, H.Y. Cheng, C. Xu, D. Sheng, Surface characteristics of crop-residue-derived black carbon and lead(II) adsorption, *Water Res.*, 42 (2008) 567–574.
- [3] X.C. Chen, G.C. Chen, L.G. Chen, Y.X. Chen, J. Lehmann, M.B. McBride, A.G. Hay, Adsorption of copper and zinc by biochars produced from pyrolysis of hardwood and corn straw in aqueous solution, *Bioresour. Technol.*, 102 (2011) 8877–8884.
- [4] K. Komnitsas, D. Zaharaki, G. Bartzas, G. Kaliakatsou, A. Kritikaki, Efficiency of pecan shells and sawdust biochar on Pb and Cu adsorption, *Desal. Wat. Treat.*, 57 (2016) 3237–3246.
- [5] D. Kolodynska, R. Wnetrzak, J.J. Leahy, M.H.B. Hayes, W. Kwapinski, Z. Hubicki, Kinetic and adsorptive characterization of biochar in metal ions removal, *Chem. Eng. J.*, 197 (2012) 295–305.
- [6] X.L. Dong, L.Q. Ma, Y.C. Li, Characteristics and mechanisms of hexavalent chromium removal by biochar from sugar beet tailing, *J. Hazard. Mater.*, 190 (2011) 909–915.
- [7] H.Y. Wang, B. Gao, S.S. Wang, J. Fang, Y.W. Xue, K. Yang, Removal of Pb(II), Cu(II), and Cd(II) from aqueous solutions by biochar derived from KMnO₄ treated hickory wood, *Bioresour. Technol.*, 197 (2015) 356–362.
- [8] H.M. Jin, S. Capareda, Z.Z. Chang, J. Gao, Y.D. Xu, J.Y. Zhang, Biochar pyrolytically produced from municipal solid wastes for aqueous As(V) removal: adsorption property and its improvement with KOH activation, *Bioresour. Technol.*, 169 (2014) 622–629.
- [9] J. Meng, X.L. Feng, Z.M. Dai, X.M. Liu, J.J. Wu, J.M. Xu, Adsorption characteristics of Cu(II) from aqueous solution onto biochar derived from swine manure, *Environ. Sci. Pollut. Res. Int.*, 21 (2014) 7035–7046.
- [10] C.C. Kung, F. Kong, Y. Choi, Pyrolysis and biochar potential using crop residues and agricultural wastes in China, *Ecol. Indic.*, 51 (2015) 139–145.
- [11] A. Bogusz, P. Oleszczuk, R. Dobrowolski, Application of laboratory prepared and commercially available biochars to adsorption of cadmium, copper and zinc ions from water, *Bioresour. Technol.*, 196 (2015) 540–549.
- [12] Q.M. Cheng, Q. Huang, S. Khan, Y.J. Liu, Z.N. Liao, G. Li, Y.S. Ok, Adsorption of Cd by peanut husks and peanut husk biochar from aqueous solutions, *Ecol. Eng.*, 87 (2016) 240–245.
- [13] J.H. Park, Y.S. Ok, S.H. Kim, J.S. Cho, J.S. Heo, R.D. Delaune, D.C. Seo, Competitive adsorption of heavy metals onto sesame straw biochar in aqueous solutions, *Chemosphere*, 142 (2016) 77–83.
- [14] R. Elangovan, L. Philip, K. Chandraraj, Biosorption of chromium species by aquatic weeds: kinetics and mechanism studies, *J. Hazard. Mater.*, 152 (2008) 100–112.
- [15] T. Chen, Z.Y. Zhou, S. Xu, H.T. Wang, W.J. Lu, Adsorption behavior comparison of trivalent and hexavalent chromium on biochar derived from municipal sludge, *Bioresour. Technol.*, 190 (2015) 388–394.
- [16] F.S. Zhou, H. Wang, S.E. Fang, W.H. Zhang, R.L. Qiu, Pb(II), Cr(VI) and atrazine sorption behavior on sludge-derived biochar: role of humic acids, *Environ. Sci. Pollut. Res.*, 22 (2015) 16031–16039.
- [17] Y. Ma, W.J. Liu, N. Zhang, Y.S. Li, H. Jiang, G.P. Sheng, Polyethylenimine modified biochar adsorbent for hexavalent chromium removal from the aqueous solution, *Bioresour. Technol.*, 169 (2014) 403–408.
- [18] L. Dupont, J. Bouanda, J. Ghanbaja, J. Dumonceau, M. Aplincourt, Use of analytical microscopy to analyze the speciation of copper and chromium ions onto a low-cost biomaterial, *J. Colloid Interface Sci.*, 279 (2004) 418–424.
- [19] J.H. Yuan, R.K. Xu, H. Zhang, The forms of alkalis in the biochar produced from crop residues at different temperatures, *Bioresour. Technol.*, 102 (2011) 3488–3497.
- [20] J.S. Noh, J.A. Schwarz, Estimation of the point of zero charge of simple oxides by mass titration, *J. Colloid Interface Sci.*, 130 (1989) 157–164.
- [21] L. Tschansky, E.R. Graber, Methodological limitations to determining acidic groups at biochar surfaces via the Boehm titration, *Carbon*, 66 (2014) 730–733.
- [22] P. Miretzky, A.F. Cirelli, Cr(VI) and Cr(III) removal from aqueous solution by raw and modified lignocellulosic materials: a review, *J. Hazard. Mater.*, 180 (2010) 1–19.
- [23] S.B. Deng, Y.P. Ting, Polyethylenimine-modified fungal biomass as a high-capacity biosorbent for Cr(VI) anions: sorption capacity and uptake mechanisms, *Environ. Sci. Technol.*, 39 (2005) 8490–8496.
- [24] X.S. Wang, Z.Z. Li, S.R. Tao, Removal of chromium (VI) from aqueous solution using walnut hull, *J. Environ. Manage.*, 90 (2009) 721–729.
- [25] H. Gao, Y.G. Liu, G.M. Zeng, W.H. Xu, T. Li, W.B. Xia, Characterization of Cr(VI) removal from aqueous solutions by a surplus agricultural waste—rice straw, *J. Hazard. Mater.*, 150 (2008) 446–452.
- [26] D.D. Maksin, A.B. Nastasovic, A.D. Milutinovic-Nikolic, L.T. Surucic, Z.P. Sandic, R.V. Hercigonja, A.E. Onjia, Equilibrium and kinetics study on hexavalent chromium adsorption onto diethylene triamine grafted glycidyl methacrylate based copolymers, *J. Hazard. Mater.*, 209–210 (2012) 99–110.
- [27] D.H. Park, S.R. Lim, Y.S. Yun, J.M. Park, Reliable evidences that the removal mechanism of hexavalent chromium by natural biomaterials is adsorption-coupled reduction, *Chemosphere*, 70 (2007) 298–305.

- [28] G.K. Choppala, N.S. Bolan, M. Megharaj, Z. Chen, R. Naidu, The influence of biochar and black carbon on reduction and bioavailability of chromate in soils, *J. Environ. Qual.*, 41 (2012) 1–10.
- [29] W.C. Ding, X.L. Dong, M. Inyang, B. Gao, L.Q. Ma, Pyrolytic temperatures impact lead sorption mechanisms by bagasse biochars, *Chemosphere*, 105 (2014) 68–74.
- [30] M. Ahmad, S.S. Lee, X.M. Dou, D. Mohan, J.K. Sung, J.E. Yang, Y.S. Ok, Effects of pyrolysis temperature on soybean stover- and peanut shell-derived biochar properties and TCE adsorption in water, *Bioresour. Technol.*, 118 (2012) 536–544.
- [31] Y. Wang, Y.T. Hu, X. Zhao, S.Q. Wang, G.X. Xing, Comparisons of biochar properties from wood material and crop residues at different temperatures and residence times, *Energy Fuels*, 27 (2013) 5890–5899.
- [32] Y.F. Xu, Z.J. Lou, P. Yi, J.Y. Chen, X.L. Ma, Y. Wang, M. Li, W. Chen, Q. Liu, J.Z. Zhou, J. Zhang, G.R. Qian, Improving abiotic reducing ability of hydrothermal biochar by low temperature oxidation under air, *Bioresour. Technol.*, 172 (2014) 212–218.
- [33] C. Djilani, R. Zaghoudi, A. Modarressi, M. Rogalski, F. Djazi, A. Lallam, Elimination of organic micropollutants by adsorption on activated carbon prepared from agricultural waste, *Chem. Eng. J.*, 189–190 (2012) 203–212.
- [34] X.L. Dong, L.Q. Ma, Y.J. Zhu, Y.C. Li, B.H. Gu, Mechanistic investigation of mercury sorption by Brazilian pepper biochars of different pyrolytic temperatures based on X-ray photoelectron spectroscopy and flow calorimetry, *Environ. Sci. Technol.*, 47 (2013) 12156–12164.
- [35] D. Mohan, C.U. Pittman, P.H. Steele, Pyrolysis of wood/biomass for bio-oil: a critical review, *Energy Fuels*, 20 (2006) 848–889.

Supplementary materials

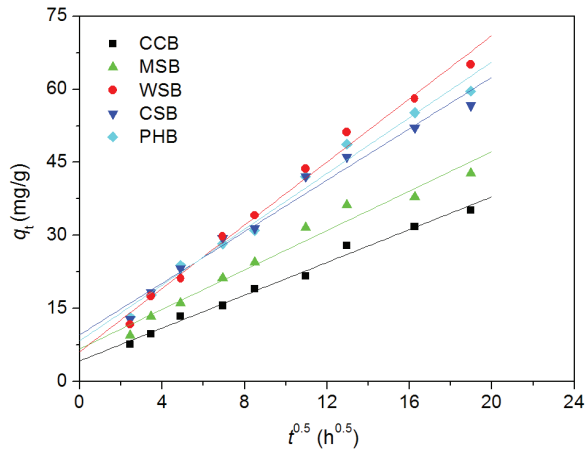


Fig. S1. Intraparticle diffusion model fitting lines of Cr adsorption kinetics.

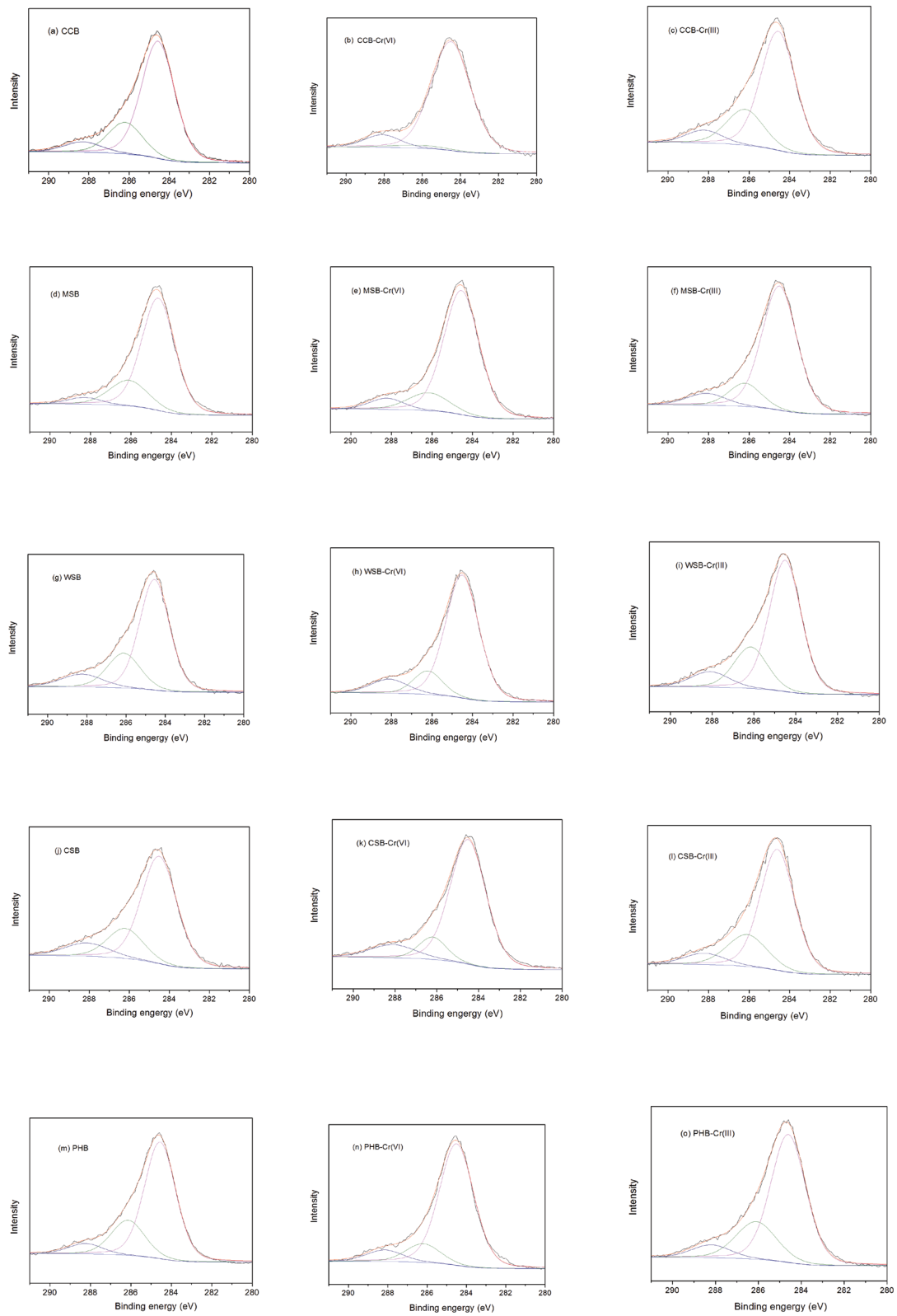


Fig. S2. Curve-fitting lines of C1s for various biochar samples.